Physiologia Plantarum

ORIGINAL RESEARCH OPEN ACCESS

The Taproot Acts as a Storage Organ During Rapeseed Vernalization

Maxence James[1] | Céline Masclaux-Daubresse[2] | Didier Goux[3] | Lun Jing[4] | Philippe Etienne[1] | Jacques Trouverie[1]

[1]Université de Caen Normandie, UNICAEN, INRAE, UMR 950 EVA, SFR Normandie Végétal (FED4277), Caen, France | [2]Institut Jean-Pierre Bourgin, INRAE, AgroParisTech, CNRS, Université Paris-Saclay, Versailles, France | [3]Université de Caen Normandie, UNICAEN, CMAbio3, US EMerode, Caen, France | [4]Centre Mondial de L'Innovation, Groupe Roullier, Saint-Malo, France

Correspondence: Maxence James (maxence.james@slu.se)

Received: 15 February 2025 | **Revised:** 25 April 2025 | **Accepted:** 7 May 2025

Handling Editor: C. Bellini

Funding: This work was supported by the Agence Nationale de la Recherche (ANR-19-CE14-0009-02 hAPPEN: Autophagy, Proteases, and plant Performances).

Keywords: ionome | oilseed rape | proline | root proteome | starch

ABSTRACT

In winter oilseed rape (*Brassica napus* L.), vernalization, prolonged cold exposure, is essential for spring flowering. Although transcriptomic changes in leaves during vernalization are studied, the taproot, a key storage organ, remains unexplored. Recently, high nitrogen (N) and carbon (C) compound levels were observed in the taproot post-vernalization, suggesting potential metabolic activities in this organ during this period. To decipher this, an integrative study combining morphological, ionomic, proteomic, and targeted biochemical analysis was conducted. This study revealed that the taproot is the only compartment that shows net gain in biomass during vernalization and confirmed its role in storing C and N reserves. A comparative proteomic analysis between the beginning and the end of the vernalization period showed that this storage is the result of a strong modulation of proteins involved in N and C metabolisms. Additionally, the up-accumulation of proteins involved in the starch and amino acid metabolisms is consistent with the increase in the starch and amino acid amounts in the taproot during vernalization. Amino acids from the glutamine family are especially accumulated, with proline being the most over-accumulated (127-fold), highlighting the initiation of a protective metabolism in the taproot during the cold stress period related to vernalization. This study also reveals the storage of macro- and microelements, notably iron, copper, and zinc. These findings provide a deeper understanding of the development and maintenance of specific metabolic activities in the taproot of *B. napus* during vernalization, ensuring the accumulation of essential N and C reserves for subsequent growth and development.

1 | Introduction

Oilseed rape (*Brassica napus* L.) is one of the three main oilseed crops in the world used for both human and animal food (Avice and Etienne 2014). In temperate regions, winter oilseed rape varieties are preferred due to their high yield and their root system, characterized by the presence of a taproot with a potential role as a storage organ, which improves soil stabilization during winter (Thomas et al. 2016; James et al. 2025). During this season, a drop in temperatures slows down and eventually leads to a cessation of growth in winter oilseed rape, initiating a period of vegetative rest when the plant is exposed

Philippe Etienne and Jacques Trouverie contributed equally to this study.

to a daily average temperature of less than 5°C for at least six consecutive days (Murphy and Scarth 1994). Moreover, unlike spring rapeseed, whose flowering does not depend on the duration and intensity of the cold period, or other *B. napus* subspecies such as *B. napus* ssp. *napobrassica*, whose flowering depends on duration but is independent of winter hardness, winter rapeseed needs both a long (6–0 weeks) and intense cold period to induce, synchronize, and accelerate spring flowering (Chouard, 1960; Schiessl 2020). During vernalization, winter oilseed rape can withstand temperatures even below −20°C without affecting its growth or grain yield (Merrien and Pouzet 1988). Vernalization requires specific metabolic changes, which have been particularly well-studied in the leaves of *Arabidopsis thaliana* (Michaels and Amasino 2000). Thus, in Brassicaceae leaves, the vernalization period triggers intricate regulatory processes, including transcriptional, and epigenetic regulation (O'Neill et al. 2019; Schiessl et al. 2019; Ahn et al. 2024). Several studies have reported that in *Arabidopsis thaliana* leaves, low temperatures associated with vernalization are characterized by the induction of proteins such as VERNALIZATION 2 (VRN2) and VERNALIZATION-INSENSITIVE 3 (VIN3) (Sung and Amasino 2004; Wood et al. 2006). These proteins form a complex responsible for the epigenetic repression of the FLOWERING LOCUS C (FLC), a key repressor of the floral transition in Brassicaceae (Sung and Amasino 2004; Schmitz and Amasino 2007; O'Neill et al. 2019; Schiessl et al. 2019). Compared to leaves, metabolic changes in roots during the vernalization period are less well documented. In sugar beet, known for its high sucrose accumulation in the taproot, Rodrigues et al. (2020) showed that vernalization induces transcriptomic and functional reprogramming, leading to the taproot's transition from a sink state to a carbohydrate source state. In *Raphanus sativus* L., transcriptomic analysis of the taproot revealed that many genes related to glucosinolates (GLS) biosynthesis were significantly downregulated during vernalization, resulting in an approximately three-fold decrease in the GLS levels in the roots (Nugroho et al. 2021). Most research provides an overview of the root states at the end of the vernalization period, focusing on their importance during subsequent developmental stages rather than on the vernalization period itself. For example, in *B. napus*, it was shown that by the end of vernalization, the taproot accumulates significant amounts of starch and proteins, indicating its potential role as a storage organ (Rossato et al. 2002; James et al. 2025). These nitrogen (N) reserves are remobilized to seeds during seed filling, highlighting the critical role of the taproot in seed development and maturity (Rossato et al. 2001).

A better understanding of the nature and function of molecules stored in the taproot as well as the metabolic pathways involved in their biosynthesis during vernalization could help optimize the agronomic performance of winter oilseed rape. To investigate this, rapeseed plants were grown under hydroponic conditions and subjected to limiting-nitrogen conditions during the vernalization period (60 days at 4°C). The nitrogen-limiting conditions were used to mimic field conditions during winter, where low temperatures impair rapeseed's N uptake capacity and reduce soil N availability due to the inhibition of bacterial nitrification (Malagoli et al. 2004; Sahoo 2022). At the beginning and end of vernalization, an integrative study was conducted, combining morphological, targeted biochemical (starch, proteins and amino acids), ionomic profiling, and proteomic analysis.

2 | Material and Methods

Seeds of *B. napus* var. Aviso were germinated for 4 days in the dark, followed by 6 days under natural light. When the first real leaf has appeared, seedlings were transferred to a 10-L tank (10 seedlings per tank) containing Hoagland solution (3.75 mM NO_3^-) composed of 1.25 mM $Ca(NO_3)_2.4H_2O$, 1.25 mM KNO_3, 0.5 mM $MgSO_4$, 0.25 mM KH_2PO_4, 0.2 mM EDTA-2NaFe-3H_2O, 14 μM H_3BO_3, 5 μM $MnSO_4$, 3 μM $ZnSO_4$, 0.7 μM $(NH_4)_6Mo_7O_{24}$, 0.7 μM $CuSO_4$, and 0.1 μM $CoCl_2$. The nutrient solution was renewed every week for 22 days. Thirty-two days after sowing (DAS), plants were transferred to low N condition (LN; 4.2 μM N) to mimic the low Navailability in soils during winter. The plants were grown in greenhouse conditions with a thermoperiod of 20°C/17°C (day/night) and a 16-h photoperiod. They were exposed to natural light, supplemented by high-pressure sodium lamps (Philips, MASTER Green Power T400W), providing an average photosynthetically active radiation of 350 μmol photons $m^{-2}s^{-1}$ at canopy height. At 47 DAS (T0), the plants were subjected to 60 days of vernalization in a climatic chamber set at 4°C, with artificial light during the day (10 h day/14 h night).

Plants were harvested at the beginning of the vernalization (T0) and at its end (108 DAS; T1). Two-millimeter taproot sections were collected for microscopic observation, whereas part of the root tissue was frozen in liquid N and stored at −80°C for subsequent biochemical analysis. The remaining portions were dried in an oven (60°C for 4 days) to determine dry weight.

2.1 | Microscopy Observations

Microscopic observations were performed as previously described by James et al. (2025). Briefly, taproot sections fixed with 2.5% glutaraldehyde in 0.1 M phosphate buffer pH 7 for 1 h to several days at 4°C were rinsed in 0.1 M phosphate buffer pH 7 three times. After dehydration in a progressive bath of ethanol (70%–100%), sections were embedded in resin EMbed 812 and polymerized for 48 h at 60°C. Then, 1 μm semi-fine sections were cut with an ultramicrotome and stained with 0.5% toluidine blue (1% sodium borate). Observations were performed using a classical light microscope (Olympus AX70 and Olympus SC30 camera).

2.2 | Elemental Analysis

Dried taproot samples were ground to a fine powder using stainless steel beads in an oscillating grinder (Mixer Mill MM400, Retsch). As detailed previously by Maillard et al. (2016), the macronutrient (Mg, P, S, Ca, and K) and micronutrient (Na, Mo, Mn, Fe Co, Ni, Cu, Zn, B, and Si) contents were quantified after acid digestion of dry weight samples (about 40 mg) with high-resolution inductively coupled plasma mass spectrometry (HR-ICP-MS, Element 2TM,

Thermo Scientific) and using internal and external standards. For N content determination, 2 mg of dried powder was analyzed using an elemental analyzer (EA3000, EuroVector).

2.3 | Extraction and Quantification of Soluble Proteins

Soluble proteins were extracted from 200 mg of frozen fresh taproot tissue ground in a mortar with 50 mg of PVPP and 300 µL of McIlvaine buffer citrate–phosphate buffer (20 mM citrate, 160 mM phosphate, pH 6.8; McIlvaine 1921). After centrifugation at 20,000 *g* at 4°C for 20 min, the supernatant was recovered and the concentrations of the soluble proteins were determined using the Bradford method (Bradford 1976) with a calibration curve of bovine serum albumin (BSA).

2.4 | Shotgun Proteomic Analysis

Protein extraction was conducted using the Phenol Extraction method described by Belouah et al. (2020). The protein pellets were subsequently solubilized with 6 M Urea, 2 M Thiourea, 30 mM TRIS–HCL (pH 8.5), 10 mM DTT, and 0.1% Rapigest (Waters). Protein concentration was measured using the 2D QuantKit (GE Healthcare) and adjusted to 2 µg/µL. A total of 20 µg of protein was then digested and desalted as described in Belouah et al. (2020).

A total of 400 ng of desalted peptide digest was injected into a Thermo Q Exactive Plus (Thermo) coupled to an Eksigent nanoLC ultra 2D (see Data S1 for detailed parameters). Peptide identification was performed using Xtandem (piledriver 2015.04.01.1) against *B. napus* refseq genome (https://www.ncbi.nlm.nih.gov/protein/?term=txid3708[Organism:exp]) and an in-house protein contaminant database (55 Entries) as described in Balliau et al. (2018). Detailed parameters are provided in Data S2.

Protein inference and quantification were conducted using i2masschroq software (http://pappso.inrae.fr/bioinfo/i2maschroq/; Langella et al. 2017; Valot et al. 2011). The protein Evalue was set to 0.00001 with two distinct peptides with an *E*-value of 0.01, resulting in a fdr of 0.1 at psm level, 0.11 at peptide level, and 0.015 at protein level. Quantification was performed as described in Balliau et al. (2018). For extracted ion chromatogram (XIC) quantification, peptides were retained if they were present in at least 90% of samples, and if the correlation for all peptides related to a protein had a correlation greater than 0.5. When the peptides of a protein were not present or not reproducibly observed in one or more conditions, spectral counting (SC) was used in place of XICs analysis. For SC quantification, proteins were retained if observed in a minimum of 5 spectra in a single sample. The mass spectrometry proteomics data have been deposited in the ProteomeXchange Consortium via the PRIDE (Perez-Riverol et al. 2022) partner repository with the dataset identifier PXD050894.

2.5 | Proteomic Data: Statistics and Data Mining

Statistical analyzes were performed using Perseus software (https://maxquant.net/perseus/). Global proteomic data were analyzed using ANOVA with developmental stage as the variable factor. For protein quantification by the XICs and SC methods, statistical analyzes were conducted on log2-transformed protein abundance. Proteins with a Student test FDR ≤0.05 were considered significantly differentially accumulated. A Fold-Change (FC) threshold of 1.5 was applied. Missing data for proteins analyzed by the SC method were imputed from a normal distribution. Gene Ontology (GO) was obtained from the panther database (pantherdb.org).

GO enrichment analyzes for the Biological Process (BP) ontology were performed on protein lists using the Cytoscape (v3.9.1) plug-in ClueGO (v2.5.9) (Bindea et al. 2009) with the *B. napus*

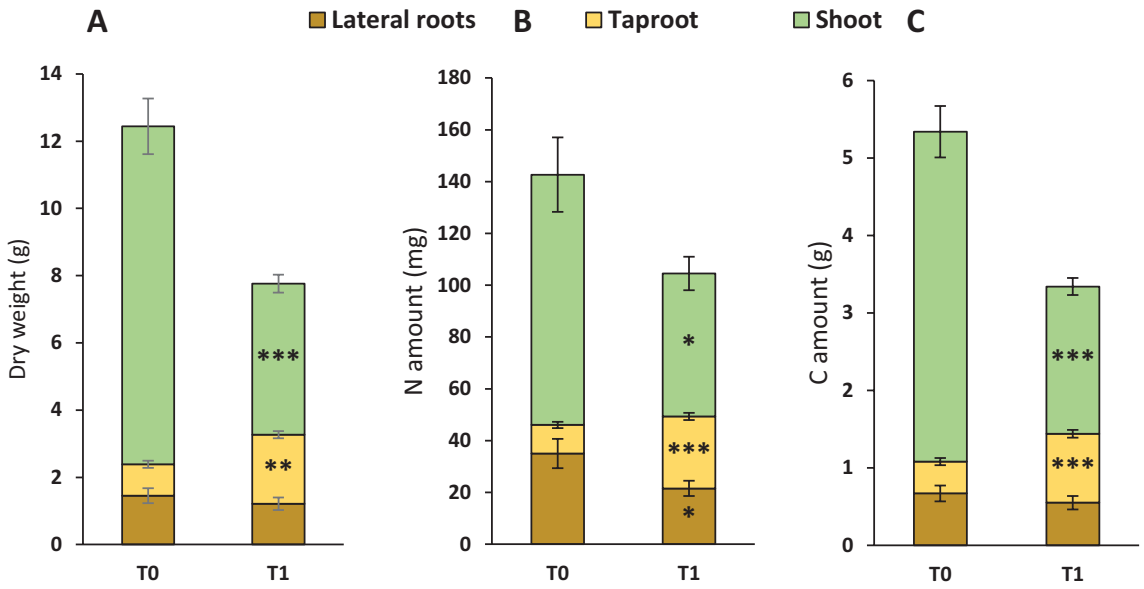

FIGURE 1 | Changes of biomasses (A) and nitrogen (B) and carbon (C) contents in shoot and roots of rapeseed between the beginning (T0) and the end (T1) of the vernalization. Results are means ± SE ($n = 4$). Significant differences between T0 and T1 are indicated by **(p value ≤0.01) and ***(p value ≤0.001).

L. genome as a background. Results focused on terms with a p value <0.05.

2.6 | Determination of Amino Acid Concentrations

For amino acid extraction, 10 mg of fresh matter lyophilized was mixed with a solution containing 400 mL of MeOH and 0.250 nmol/mL of Norvaline (Sigma Aldrich) used as the internal standard. The extract was stirred for 15 min and re-suspended with 200 mL of chloroform (agitation for 5 min) and 400 mL of double-distilled water (ddH_2O). After centrifugation (18,500 g, 10°C, 5 min), the supernatant was recovered, evaporated, and dissolved in 100 mL of ddH_2O. Derivatization was performed using an Ultra Derivatization Kit AccQ tag (Waters Corp), following the protocol of the manufacturer. The amino acid profile was determined by ultra-performance liquid chromatography coupled with a photodiode array detector (UPLC/PDA) H-Class system (Waters Corp) with an ethylene bridge hybrid (BEH) C18 100 × 2.1 mm column (pore size: 1.7 mm).

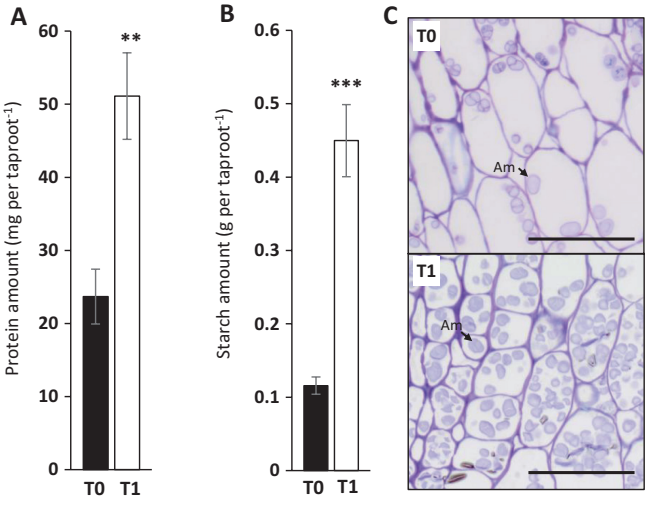

FIGURE 2 | Changes of soluble protein (A), starch (B), and tissue structure (C) in taproot of rapeseed at the beginning (T0) and the end (T1) of the vernalization. Am: Amyloplast. Black scale corresponds to 50 μm. Values are means ± SE ($n = 4$). Significant differences between T0 and T1 are indicated by **(p value ≤ 0.01) and ***(p value ≤ 0.001).

2.7 | Determination of Starch Concentrations

Starch was quantified from 50 mg of lyophilized material using the Total Starch enzymatic kit (Megazyme International). Briefly, starch was digested first with thermal stable α-amylase and then with amyloglucosidase after gelatinization at 100°C. The glucose units released from starch hydrolysis were measured spectrophotometrically at 510 nm using glucose oxidase/peroxidase and 4-aminoantipyrine (GOPOD reagent) and glucose as a standard. Weight of free glucose was converted to anhydroglucose using a multiplication factor of 162/180.

2.8 | Statistical Analyzes

For all parameters, at least three biological replicates were measured ($n \geq 3$). All data are presented as mean ± standard error (SE). To compare different data between different times (T0 and T1), Tukey tests were performed after verifying compliance of normality with the Shapiro–Wilk test with *R* software. When the data did not conform to the normal distribution, they were transformed into Log. Statistical significance was postulated at $p \leq 0.05$.

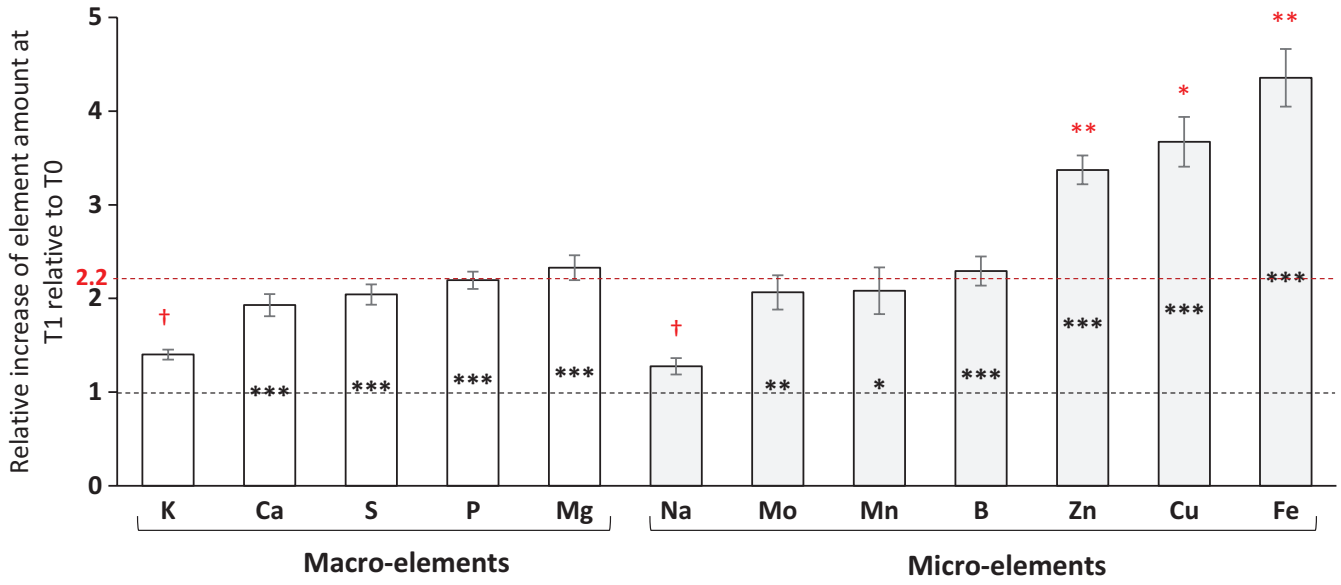

FIGURE 3 | Increase of macro- and micro-element amounts in taproot of rapeseed at the end (T1) of the vernalization relative to the beginning (T0). Elements significantly accumulated in taproot at T1 have a ratio over 1 (doted black line) and are indicated by black asterisks (*p value ≤ 0.05, **p value ≤ 0.01, and ***p value ≤ 0.001). Elements with a ratio significantly higher or lower than the taproot biomass ratio between T0 and T1 (2.2: Doted red line) are over-concentrated (red asterisks; *p value ≤ 0.05, **p value ≤ 0.01) and under-concentrated (†p value ≤ 0.05), respectively. Results are means ± SE ($n = 4$).

3 | Results

3.1 | The Taproot Is a Storage Organ During Vernalization

Whole-plant dry biomass decreased from 12.5 g at the beginning of vernalization (T0) to 7.8 g at its end (T1), reflecting a 55.3% biomass loss in the leaf compartment at T1, mainly due to leaf drop (Tables S1–S5; Figures 1A and S1). This reduction in leaf biomass led to a proportional decrease in N content (43%) and in carbon (C) content (55.4%) (Figure 1B,C).

In contrast, total root dry biomass increases during the same period, a 2.2-fold increase in taproot dry biomass while lateral root dry biomass remained unchanged (Figure 1A). In the same way, the amounts of N and C in the taproot increase in proportion to biomass, with 2.5- and 2.2-fold rises, respectively (Figure 1B,C). Overall, these results show that the taproot is the main storage organ for N and C during vernalization. Thus, the accumulation of main organic N (proteins) and C (starch) storage compounds was explored. Between the entry (T0) and at the end of vernalization (T1), the soluble protein amount in the taproot increased from 23.7 ± 3.8 to 51.1 ± 5.9 mg (Figure 2A). Starch was also over-accumulated, increasing 3.9-fold during vernalization, consistent with the observed increase in the number and size of amyloplasts in taproot cells over the same period (Figure 2B,C).

Beyond C and N, the effect of vernalization on the amount of key macroelements (K, Ca, S, P, Mg) and microelements (Na, Mo, Mn, Fe, Ni, Cu, Zn, B) in the taproot was also explored (Figure 3). Among these, K and Na were the only elements whose amounts did not change significantly, leading to a decrease in their concentrations (−35% and −41% for K and Na, respectively) due to the increase in taproot biomass (Figures 3 and S1). Conversely, elements such as Ca, S, P, Mg, Mo, Mn, and B accumulated in the taproot at a rate similar to the taproot biomass increase (2.2-fold) during vernalization. Meanwhile, Zn, Cu, and Fe were the most highly accumulated microelements, as their amounts increased more than the taproot biomass, resulting in higher concentrations of 151.1 ± 9.6, 168.1 ± 19.7, and 190.4% ± 16%, respectively (Figure 3; Table S1).

3.2 | Pathways Related to Stress Response and N and C Storage Are Exacerbated in Taproot During Vernalization

Considering the elemental storage capacity of the taproot during vernalization, a shotgun proteomic analysis was carried out to identify metabolic modifications contributing to this process. Overall, the proteomic analysis revealed that between the beginning (T0) and the end (T1) of the vernalization, 788 proteins were differentially accumulated (DAPs), with 301 up-accumulated and 487 down-accumulated, respectively (Figure 4A; Tables S2 and S3).

The GO enrichment analysis of under-accumulated DAPs (Figure 4B; Table S4) highlighted biological processes primarily associated with vesicular transport (GO:0006891: intra-Golgi vesicle-mediated transport, GO:0016192: vesicle-mediated transport, GO:0048193: Golgi vesicle transport, GO:0006888: endoplasmic reticulum to Golgi vesicle-mediated transport, GO:0051693: actin filament capping, GO0051017: actin filament bundle assembly, GO:0006890: retrograde vesicle-mediated transport, Golgi to endoplasmic reticulum) and aromatic amino acid metabolism (GO:0009072: aromatic amino acid family metabolic). Similarly, the GO enrichment analysis of DAPs

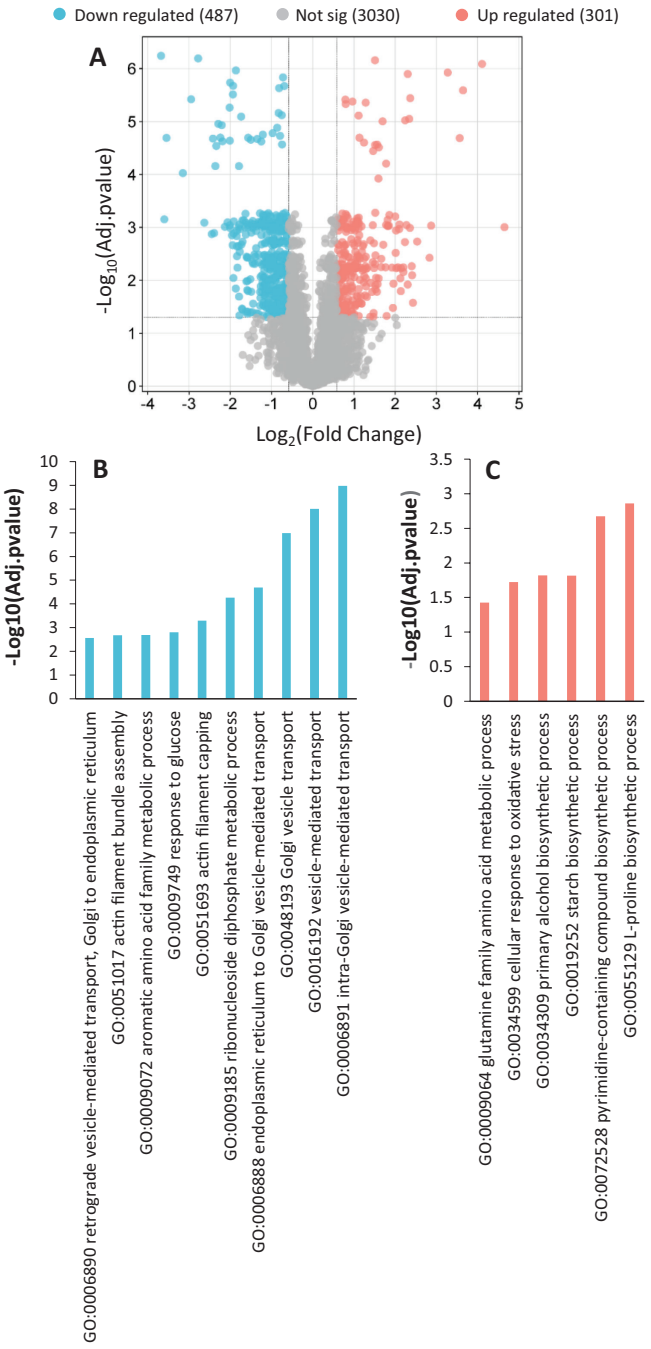

FIGURE 4 | Identification of proteins differentially abundant in taproot at the beginning and the end of vernalization. The proteins significantly accumulated (red) or depleted in taproot at the end of vernalization (T1) compared to the beginning of vernalization (T0) are represented (A). The volcanoplot corresponds to all the proteins identified by MS. Cutoffs were applied at a Fold-change of 1.5 and an adj. *p* value of 0.05. Enrichment in GO terms for biological processes is presented for the over-accumulated (B) and the depleted (C) proteins. In (B) and (C), histogram bars correspond to the top 10 of the enriched biological processes.

over-accumulated (Figure 4C; Table S5) highlights biological processes mainly related to glutamine family amino acid metabolism (GO:0055129: proline biosynthesis process and GO:0009064: glutamine family amino acid metabolic process), carbon metabolism (GO:0019252: starch biosynthetic process) and stress response (GO:0034599: cellular response to oxidative stress).

The strong enrichment of GO terms related to amino acid biosynthesis led to a broad spectrum quantification of amino acids (Figure 5). Total amino acid content increased by 3-fold between T0 and T1. Specifically, proline, glutamate, glutamine, aspartate-arginine, valine, and asparagine significantly accumulated in the taproot during vernalization. Notably, among amino acids of the glutamine family, proline, glutamate, glutamine, and aspartate-arginine were the most accumulated, with a 127-, 3.78-, 2.11-, and 6.12-fold increases, respectively (Figure 5). These accumulations resulted in elevated concentrations of proline, aspartate-arginine, valine, and asparagine in the taproot at the end of vernalization. In contrast, GABA, alanine, threonine, tyrosine, and glycine, whose levels remained relatively stable, were found at a lower level in the taproot at T1 compared to T0 (Figures 5 and S2).

Given the substantial proline accumulation (127-fold) and the enrichment of GO terms related to amino acids, particularly proline, DAPs and amino acids associated with proline metabolism were mapped onto the proline biosynthesis and catabolism pathway (Figure 6). Four proteins (XP_022556650.1, NP_001302684.1, XP_013691723.1, and XP_013716867.1) belonging to the delta-1-pyrroline-5-carboxylate synthetase family (EC:2.7.2.11 and EC:1.2.1.41), which catalyze the synthesis of L-glutamate 5-semialdehyde from glutamate and glutamine (two amino acids accumulated in the taproot), were over-accumulated during vernalization. In contrast, two proteins (XP_013643369.1 and XP_013686101.1) from the prolyl-4-hydrolase family (EC:1.14.11.2), involved in proline catabolism into 4-hydroxy-proline, were under-accumulated (Figure 6). Altogether, these metabolic modifications likely explain the observed accumulations of proline and arginine during vernalization. Similarly, a detailed analysis of the starch biosynthetic pathway was performed (Figure 7). The over-accumulation of the six DAPs (XP_013644946.1, NP_001303131.1, XP_013706820.1, XP_022568273.1, XP_013692058.1, and XP_013748431.1), mapped onto this pathway and belonging to the glucose-1-phosphate adenylyltransferase family (EC:2.7.7.27), the granule-bound starch synthase family (EC:2.4.1.242), and the 1,4-alpha-glucan branching enzyme family (EC:2.4.1.18), aligns with the increased starch content observed during vernalization (Figure 2).

4 | Discussion

4.1 | Taproot: A Crucial Storage Compartment During Vernalization

This study shows that the vernalization period temporarily decelerates the growth of winter oilseed rape (*B. napus* L.). Vernalization leads to a decrease in total dry mass due to a reduction in leaf dry mass (primarily caused by leaf drop) and a halt in lateral root growth (Figures 1 and S1). These findings align with previous studies reporting that low temperatures cause root

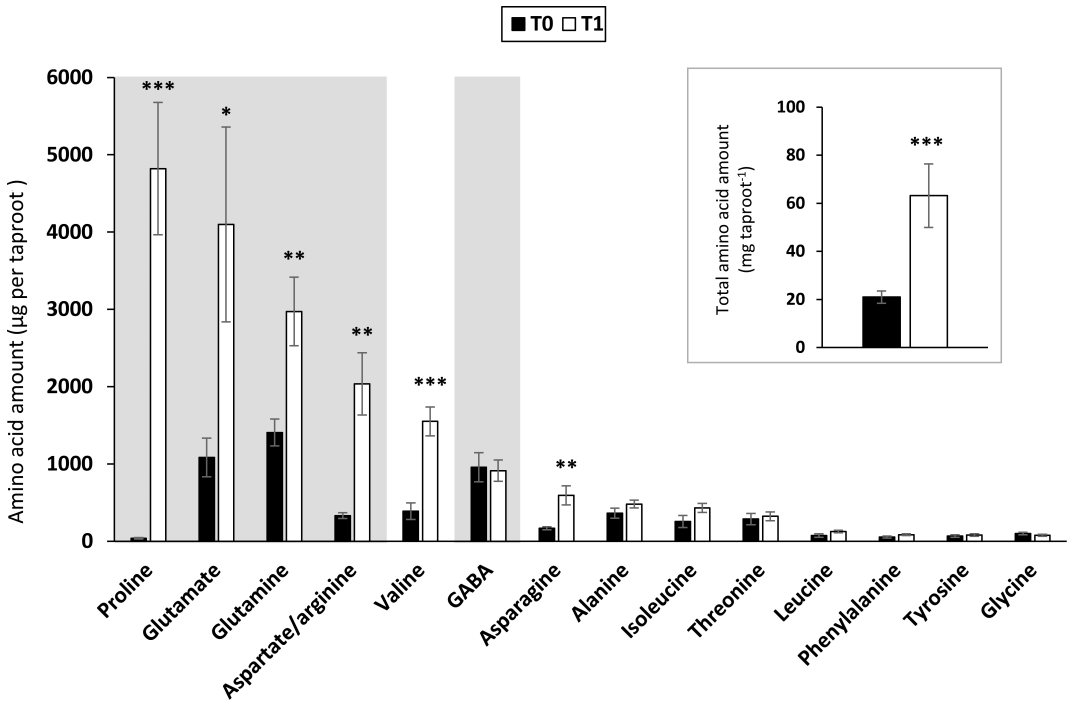

FIGURE 5 | Amino acid contents in the taproot of rapeseed at the beginning (T0) and the end (T1) of vernalization. The main figure and the insert represent the content in each and total amino acids, respectively. Amino acids on a grey background belong to the glutamine family. Significantly accumulated amino acids between T0 and T1 are indicated by *(p value ≤ 0.05), **(p value ≤ 0.01) and ***(p value ≤ 0.001). Values are means ± SE ($n = 4$).

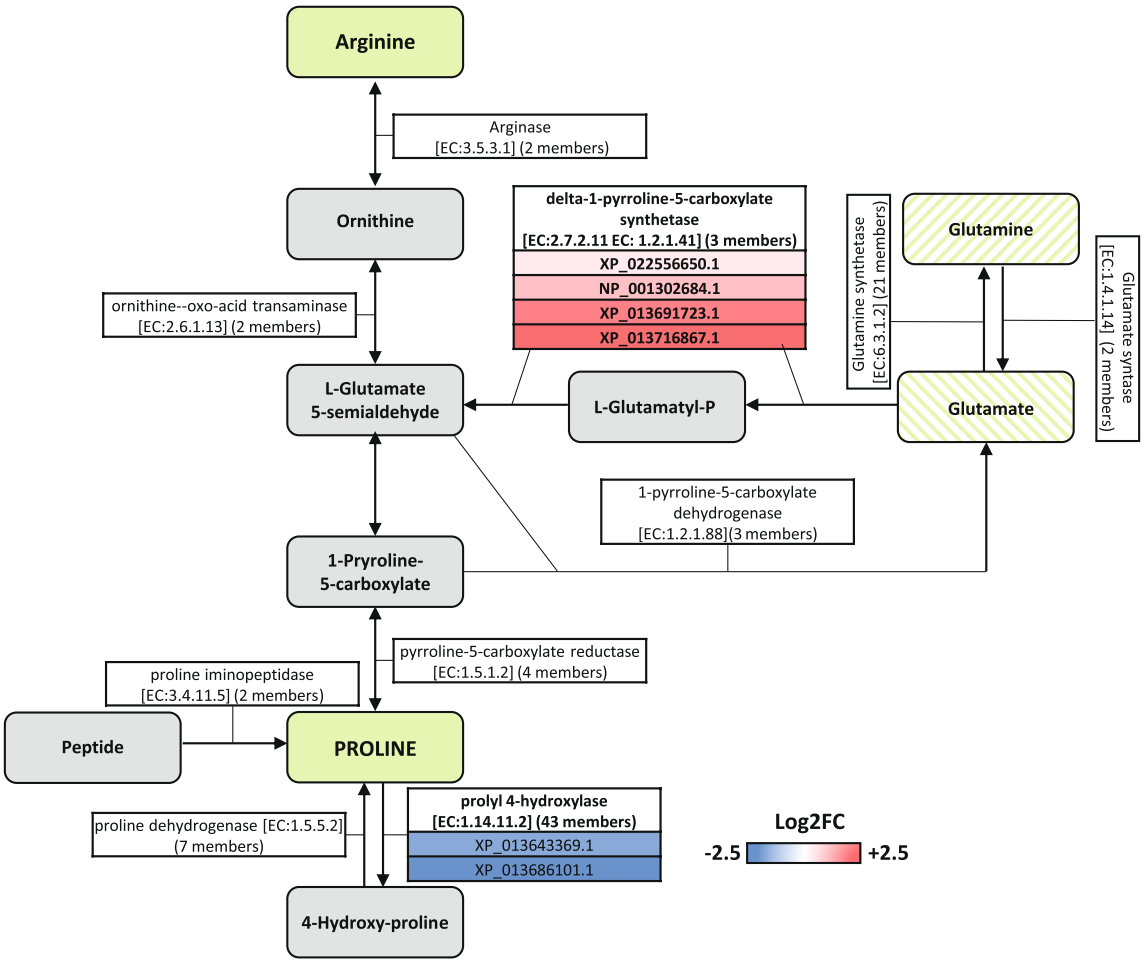

FIGURE 6 | Differentially accumulated proteins in proline biosynthetic and catabolic pathways in taproot of *Brassica napus* between the beginning (T0) and the end (T1) of vernalization. The blue to red scale is related to the Log2FC of the down- and up-accumulated enzymes (identified by their Uniprot ID), respectively. Amino acids experimentally measured to accumulate and over-accumulate during vernalization are indicated in hatched and solid green background, respectively. Metabolic pathways were adapted from KEGG database.

growth arrest in many crop plants, including *Arabidopsis thaliana* (Zhu et al. 2015; Hussain et al. 2018). In contrast, the taproot is the only plant compartment that shows a net gain in biomass, with a twofold increase between the beginning and end of vernalization. The increase in taproot biomass is associated with carbon (C) storage, as indicated by a rise in amyloplast number and a fourfold accumulation of starch, which reaches approximately 22% of the taproot dry biomass at the end of vernalization (T1) (Figure 2B,C). This low-temperature carbon storage role is also observed in other *Brassica napus* subspecies, such as *Brassica napus* L. ssp. *rapifera* Metzg., which stores carbon but mainly in the form of soluble sugars in a hypocotyl modified for this function (Johansen et al. 2016; Mølmann et al. 2021). Similarly, despite N deprivation, N content increased in the taproot, suggesting that N is remobilized from source organs (i.e., leaves and/or lateral roots) and stored primarily as proteins and amino acids, with levels increasing approximately twofold and threefold, respectively, during vernalization (Figures 2A and 5 and S2). These results are in line with previous studies reporting high starch and protein levels in the taproot at the onset of the reproductive stage, supporting its role as a buffer storage organ (Rossato et al. 2001, 2002). Interestingly, in addition to C and N, the increase in taproot biomass during vernalization facilitates the storage of most macroelements (Ca, S, P, and Mg) and microelements (Mo, Mn, B, Zn, Cu, and Fe), with certain elements, such as Zn, Cu, and Fe, being highly accumulated without showing any symptoms of toxicity (Figure 3; Table S1). Altogether, these results highlight the special role of the taproot as a key storage organ for various essential elements that can later be mobilized to support reproductive tissues. The accumulation of these compounds, particularly organic ones, raises questions about the metabolic processes that contribute to their accumulation in the taproot during vernalization.

4.2 | Proteome Modifications During Vernalization Highlight Stress Response and Storage Metabolism in the Taproot

This study reveals significant proteome modulation in the taproot during cold exposure, with 788 differentially accumulated proteins (DAPs), including 487 down-accumulated and 301 up-accumulated proteins, between the beginning and end of vernalization. Gene ontology (GO) enrichment analysis of these DAPs indicates an impact on several biological processes (Figure 4; Tables S4 and S5), including amino acid metabolism (GO:0055129: L-proline biosynthetic process, GO:0009064:

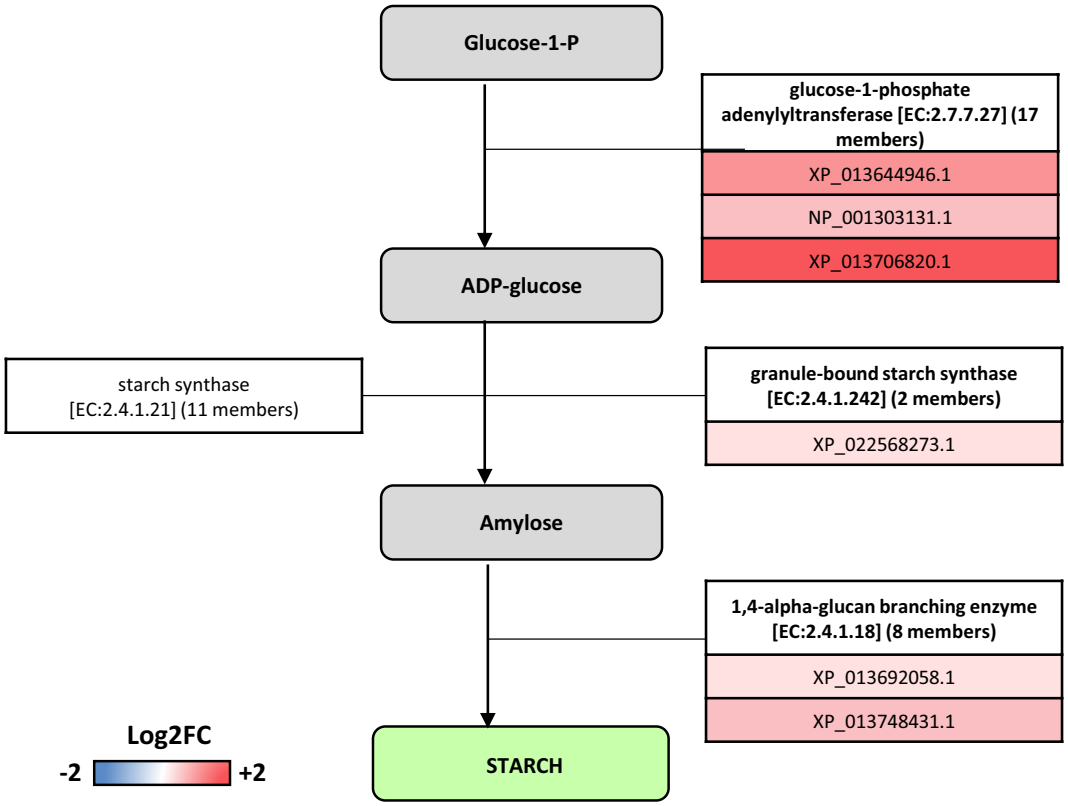

FIGURE 7 | Differentially accumulated proteins in starch biosynthetic pathway in taproot of *Brassica napus* between the beginning (T0) and the end (T1) of vernalization. The blue to red scale is related to the Log2Fc of the down- and up-accumulated enzymes (identified by their Uniprot ID), respectively. Metabolites experimentally measured to accumulate during vernalization are indicated in solid green background. Metabolic pathway was adapted from KEGG database.

glutamine family amino acid metabolic process, GO:0009072: aromatic amino acid family metabolic process). More specifically, the up-accumulated proteins (301 proteins) are primarily related to the biosynthesis of proline and other amino acids from the glutamine family, such as glutamate, glutamine, and aspartate/arginine (Figures 3 and 5). Since plants were grown under N deprivation, the accumulation of glutamine family amino acids in the taproot likely results from N remobilization from leaves. This hypothesis is supported by the absence of glutamine synthase and glutamate synthase induction during vernalization, suggesting that glutamine and glutamate accumulation is not due to neosynthesis but rather to export from leaves. This is consistent with previous studies reporting that during leaf N remobilization, asparagine, glutamate, and glutamine are the primary N and carbon transport forms in phloem sap across many plant species (Masclaux-Daubresse et al. 2010; Xu et al. 2012).

Additionally, several isoforms of delta-1-pyrroline-5-carboxylate synthetase, which catalyzes the conversion of glutamate into L-glutamate 5-semialdehyde, a precursor of arginine and proline, were over-accumulated in the taproot (Figure 6). This over-accumulation, combined with the influx of glutamine and glutamate, likely explains their high accumulation levels. Proline accumulation was particularly pronounced (127-fold; Figure 5), which can be attributed to the under-accumulation of two prolyl 4-hydroxylase isoforms involved in proline catabolism (Figure 6).

Proline, representing approximately 2% of total N in the taproot, serves as both an N and C storage compound, potentially supporting post-stress growth recovery, as previously demonstrated in *B. napus* leaves by Vartanian et al. (1992). Beyond storage, proline, along with aspartate, acts as a compatible solute, helping plants endure abiotic stresses such as salinity, drought, and cold by maintaining osmotic balance and protecting enzyme and membrane structures from oxidative damage (Naidu et al. 1991; Hayat et al. 2012; Mansour and Ali 2017; Han et al. 2021; Khan et al. 2025). The accumulation of proline and aspartate in the rapeseed taproot during vernalization may therefore contribute to preserving this organ during cold stress. Furthermore, the accumulation of all glutamine family amino acids suggests that they constitute a significant N reservoir in the taproot that can be reused after vernalization to support plant growth. In addition to amino acids, proteins, another major N storage form, are known to accumulate in taproot cortical cell vacuoles (Rossato et al. 2002). Consistently, our study shows that protein content in the taproot more than doubled during vernalization (Figure 2A). Interestingly, GO enrichment analysis of down-accumulated proteins highlighted multiple terms related to vesicular transport (GO:0006891, GO:0016192, GO:0048193, GO:0006888, GO:0051693, GO:0051017, GO:0006890; Figure 4). This compromised vesicular trafficking may indicate the activation of a Golgi bypass mechanism that facilitates unconventional protein transport to vacuoles, as previously observed in plants under stress (Sampaio et al. 2022). These reserves of amino acids and proteins function as N storage, later supporting growth and

yield during the reproductive stage, as demonstrated in *B. napus* (Rossato et al. 2001; Liang et al. 2023; James et al. 2025).

Taproot is also a C storage organ. Starch accumulation in the taproot reaches up to 22% of its dry biomass by the end of vernalization. This accumulation is paralleled by the over-accumulation of three key enzymes in the starch biosynthesis pathway: glucose-1-phosphate adenylyltransferase, granule-bound starch synthase, and 1,4-alpha-glucan branching enzyme (Figures 1 and 7).

Aromatic amino acids are synthesized from glycolytic intermediates (glucose-6-P and phosphoenol pyruvate) via the shikimate pathway (Yokoyama 2024). The under-accumulation of proteins involved in aromatic amino acid metabolism (GO:0009072; Figure 4), along with decreased phenylalanine and tyrosine concentrations in the taproot during vernalization (Figures 5 and S2), suggests a metabolic shift from glucose catabolism to starch biosynthesis. This aligns with previous studies showing that starch serves as a key C storage compound, which is utilized during the transition from vegetative to floral stages in many plant species (MacNeill et al. 2017; James et al. 2025).

4.3 | Micronutrient Storage and Stress Tolerance Mechanisms in the Taproot

In addition to N and carbon, macro- and micronutrients are stored in the taproot, with Zn, Cu, and Fe accumulating beyond biomass increase (Figures 3 and S2). Excessive Zn, Cu, and Fe can cause physiological stress, including growth reduction, nutrient uptake imbalances, and increased reactive oxygen species (ROS) production (Kaur and Garg 2021; Li et al. 2024; Xu et al. 2024). However, the continued growth of the taproot during vernalization suggests active protective mechanisms against the potential negative effects of the accumulation of these three elements. Proteomic analysis revealed the accumulation of multiple proteins associated with stress alleviation, including metal tolerance protein 1-like (Table S6), which is known to transport Zn and Fe from the cytoplasm to the vacuole, likely contributing to hypertolerance to elevated Zn and Fe concentrations (Ricachenevsky et al. 2013). The high Fe concentration observed in the taproot (Figure S3) may also be tolerated due to the accumulation of Fe-binding proteins such as ferritin (Table S6). These results are consistent with those of James et al. (2025), who reported that these proteins are present in the taproot of *B. napus* L. at the end of the vernalization period and continue to accumulate during the reproductive stage. Similarly, the accumulation of two superoxide dismutase isoforms [Cu-Zn] (Table S6) may explain the high accumulation of Cu and could be involved in its storage as well as the response to oxidative stress that could result from an accumulation of these metal ions (Dreyer and Schippers 2019). These proteins help mitigate metal toxicity, enabling Zn, Fe, and Cu storage for later use during spring growth.

5 | Conclusion

During the vernalization period, the taproot undergoes extensive metabolic remodeling to function as a storage organ for N, C, and other essential nutrients. This metabolic shift likely supports subsequent developmental stages and yield in *B. napus*. Given the importance of these reserves during the reproductive stage (James et al. 2025), future research could assess the impact of genotypic variability on taproot storage capacity and its potential impact on rapeseed growth, stress resistance, and productivity. Thus, improving N and carbon storage during vernalization could be a lever for improving rapeseed performance under low-input conditions, and thus promote more sustainable agriculture aimed at reducing the crop's environmental footprint.

Author Contributions

M.J., P.E. and J.T.: conceptualization; M.J., D.G. and L.J.: investigation; M.J.: data curation; M.J.: formal analysis; M.J., P.E., J.T. and C.M.-D.: visualization; M.J., P.E., J.T. and C.M.-D: writing – original draft preparation; D.G., L.J., C.M.-D., P.E. and J.T.: writing – review and editing; C.M.-D., P.E. and J.T.: supervision; C.M.-D., P.E.: funding acquisition.

Acknowledgments

We are most grateful to PLATIN' (Plateau d'Isotopie de Normandie) core facility for elemental analysis. Dr. Benoît Bernay from Proteogen platform for his help with proteomic analysis.

Conflicts of Interest

The authors declare no conflicts of interest.

Data Availability Statement

The mass spectrometry proteomics data were deposited at the ProteomeXchange Consortium via the PRIDE (Perez-Riverol et al. 2022) partner repository with the data set identifier PXD050894.

References

Ahn, J.-Y., S. Subburaj, F. Yan, et al. 2024. "Molecular Evaluation of the Effects of FLC Homologs and Coordinating Regulators on the Flowering Responses to Vernalization in Cabbage (*Brassica Oleracea var. Capitata*) Genotypes." *Genes* 15, no. 2: 154. https://doi.org/10.3390/genes15020154.

Avice, J.-C., and P. Etienne. 2014. "Leaf Senescence and Nitrogen Remobilization Efficiency in Oilseed Rape (*Brassica napus* L.)." *Journal of Experimental Botany* 65: 3813–3824.

Balliau, T., M. Blein-Nicolas, and M. Zivy. 2018. "Evaluation of Optimized Tube-Gel Methods of Sample Preparation for Large-Scale Plant Proteomics." *PRO* 6: 6.

Belouah, I., C. Bénard, A. Denton, et al. 2020. "Transcriptomic and Proteomic Data in Developing Tomato Fruit." *Data in Brief* 28: 105015.

Bindea, G., B. Mlecnik, H. Hackl, et al. 2009. "ClueGO: A Cytoscape Plug-In to Decipher Functionally Grouped Gene Ontology and Pathway Annotation Networks." *Bioinformatics* 25: 1091–1093.

Bradford, M. M. 1976. "A Rapid and Sensitive Method for the Quantitation of Microgram Quantities of Protein Utilizing the Principle of Protein-Dye Binding." *Analytical Biochemistry* 72: 248–254.

Chouard, P. 1960. "Vernalization and its Relations to Dormancy." *Annual Review of Plant Physiology* 11: 191–238.

Dreyer, B. H., and J. H. M. Schippers. 2019. "Copper-Zinc Superoxide Dismutases in Plants: Evolution, Enzymatic Properties, and Beyond." *Annual Plant Reviews Online* 2: 933–968.

Han, M., C. Zhang, P. Suglo, S. Sun, M. Wang, and T. Su. 2021. "L-Aspartate: An Essential Metabolite for Plant Growth and Stress Acclimation." *Molecules* 26: 1887.

Hayat, S., Q. Hayat, M. N. Alyemeni, A. S. Wani, J. Pichtel, and A. Ahmad. 2012. "Role of Proline Under Changing Environments." *Plant Signaling & Behavior* 7: 1456–1466.

Hussain, H. A., S. Hussain, A. Khaliq, et al. 2018. "Chilling and Drought Stresses in Crop Plants: Implications, Cross Talk, and Potential Management Opportunities." *Frontiers in Plant Science* 9: 393. https://doi.org/10.3389/fpls.2018.00393.

James, M., C. Masclaux-Daubresse, T. Balliau, et al. 2025. "Multi-Scale Phenotyping of Senescence-Related Changes in Roots of Rapeseed in Response to Nitrate Limitation." *Journal of Experimental Botany* 76: 312–330.

Johansen, T. J., S. F. Hagen, G. B. Bengtsson, and J. A. B. Mølmann. 2016. "Growth Temperature Affects Sensory Quality and Contents of Glucosinolates, Vitamin C and Sugars in Swede Roots (*Brassica napus* L. Ssp. *Rapifera* Metzg.)." *Food Chemistry* 196: 228–235.

Kaur, H., and N. Garg. 2021. "Zinc Toxicity in Plants: A Review." *Planta* 253: 129.

Khan, P., A. M. M. Abdelbacki, M. Albaqami, R. Jan, and K.-M. Kim. 2025. "Proline Promotes Drought Tolerance in Maize." *Biology* 14: 41.

Langella, O., B. Valot, T. Balliau, M. Blein-Nicolas, L. Bonhomme, and M. Zivy. 2017. "X! TandemPipeline: A Tool to Manage Sequence Redundancy for Protein Inference and Phosphosite Identification." *Journal of Proteome Research* 16: 494–503.

Li, G., J. Wu, H. J. Kronzucker, B. Li, and W. Shi. 2024. "Physiological and Molecular Mechanisms of Plant-Root Responses to Iron Toxicity." *Journal of Plant Physiology* 297: 154257.

Liang, G., Y. Hua, H. Chen, et al. 2023. "Increased Nitrogen Use Efficiency via Amino Acid Remobilization From Source to Sink Organs in *Brassica napus*." *Crop Journal* 11: 119–131.

MacNeill, G. J., S. Mehrpouyan, M. A. A. Minow, J. A. Patterson, I. J. Tetlow, and M. J. Emes. 2017. "Starch as a Source, Starch as a Sink: The Bifunctional Role of Starch in Carbon Allocation." *Journal of Experimental Botany* 68, no. 16: 4433–4453. https://doi.org/10.1093/jxb/erx291.

Maillard, A., P. Etienne, S. Diquélou, et al. 2016. "Nutrient Deficiencies Modify the Ionomic Composition of Plant Tissues: A Focus on Cross-Talk Between Molybdenum and Other Nutrients in *Brassica napus*." *Journal of Experimental Botany* 67: 5631–5641.

Malagoli, P., P. Lainé, E. Le Deunff, L. Rossato, B. Ney, and A. Ourry. 2004. "Modeling Nitrogen Uptake in Oilseed Rape cv Capitol During a Growth Cycle Using Influx Kinetics of Root Nitrate Transport Systems and Field Experimental Data." *Plant Physiology* 134: 388–400.

Mansour, M. M. F., and E. F. Ali. 2017. "Evaluation of Proline Functions in Saline Conditions." *Phytochemistry* 140: 52–68.

Masclaux-Daubresse, C., F. Daniel-Vedele, J. Dechorgnat, F. Chardon, L. Gaufichon, and A. Suzuki. 2010. "Nitrogen Uptake, Assimilation and Remobilization in Plants: Challenges for Sustainable and Productive Agriculture." *Annals of Botany* 105: 1141–1157.

McIlvaine, T. C. 1921. "A Buffer Solution for Colorimetric Comparison." *Journal of Biological Chemistry* 49: 183–186.

Merrien, A., and A. Pouzet. 1988. Principaux Facteurs Limitant Les Rendements de Colza D'hiver Dans Les Conditions Française Physiologie et Élaboration du Rendement du Colza D'hiver Paris: CETIOM-INRA. 16–22.

Michaels, S. D., and R. M. Amasino. 2000. "Memories of Winter: Vernalization and the Competence to Flower." *Plant, Cell & Environment* 23: 1145–1153.

Mølmann, J. A., E. Hansen, and T. J. Johansen. 2021. "Effects of Supplemental LED Light Quality and Reduced Growth Temperature on Swede (L. ssp. Rapifera Metzg.) Root Vegetable Development and Contents of Glucosinolates and Sugars." *Journal of the Science of Food and Agriculture* 101: 2422–2427.

Murphy, L. A., and R. Scarth. 1994. "Vernalization Response in Spring Oilseed Rape (*Brassica Napus* L.) Cultivars." *Canadian Journal of Plant Science* 74: 275–277.

Naidu, B. P., L. G. Paleg, D. Aspinall, A. C. Jennings, and G. P. Jones. 1991. "Amino Acid and Glycine Betaine Accumulation in Cold-Stressed Wheat Seedlings." *Phytochemistry* 30: 407–409.

Nugroho, A. B. D., S. W. Lee, A. N. Pervitasari, et al. 2021. "Transcriptomic and Metabolic Analyses Revealed the Modulatory Effect of Vernalization on Glucosinolate Metabolism in Radish (*Raphanus sativus* L.)." *Scientific Reports* 11: 24023.

O'Neill, C. M., X. Lu, A. Calderwood, et al. 2019. "Vernalization and Floral Transition in Autumn Drive Winter Annual Life History in Oilseed Rape." *Current Biology* 29: 4300–4306.

Perez-Riverol, Y., J. Bai, C. Bandla, et al. 2022. "The PRIDE Database Resources in 2022: A Hub for Mass Spectrometry-Based Proteomics Evidences." *Nucleic Acids Research* 50: D543–D552.

Ricachenevsky, F. K., P. K. Menguer, R. A. Sperotto, L. E. Williams, and J. P. Fett. 2013. "Roles of Plant Metal Tolerance Proteins (MTP) in Metal Storage and Potential Use in Biofortification Strategies." *Frontiers in Plant Science* 4: 144. https://doi.org/10.3389/fpls.2013.00144.

Rodrigues, C. M., C. Müdsam, I. Keller, et al. 2020. "Vernalization Alters Sink and Source Identities and Reverses Phloem Translocation From Taproots to Shoots in Sugar Beet." *Plant Cell* 32: 3206–3223.

Rossato, L., P. Lainé, and A. Ourry. 2001. "Nitrogen Storage and Remobilization in *Brassica napus* L. During the Growth Cycle: Nitrogen Fluxes Within the Plant and Changes in Soluble Protein Patterns." *Journal of Experimental Botany* 52: 1655–1663.

Rossato, L., C. Le Dantec, P. Laine, and A. Ourry. 2002. "Nitrogen Storage and Remobilization in *Brassica Napus* L. During the Growth Cycle: Identification, Characterization and Immunolocalization of a Putative Taproot Storage Glycoprotein." *Journal of Experimental Botany* 53: 265–275.

Sahoo, M. 2022. "Winter Soil Temperature and Its Effect on Soil Nitrate Status: A Support Vector Regression-Based Approach on the Projected Impacts." *Catena* 211: 105958.

Sampaio, M., J. Neves, T. Cardoso, J. Pissarra, S. Pereira, and C. Pereira. 2022. "Coping With Abiotic Stress in Plants—An Endomembrane Trafficking Perspective." *Plants* 11: 338.

Schiessl, S. 2020. "Regulation and Subfunctionalization of Flowering Time Genes in the Allotetraploid Oil Crop *Brassica Napus*." *Frontiers in Plant Science* 11: 605155. https://doi.org/10.3389/fpls.2020.605155.

Schiessl, S. V., D. Quezada-Martinez, E. Tebartz, R. J. Snowdon, and L. Qian. 2019. "The Vernalisation Regulator FLOWERING LOCUS C Is Differentially Expressed in Biennial and Annual *Brassica napus*." *Scientific Reports* 9: 14911.

Schmitz, R. J., and R. M. Amasino. 2007. "Vernalization: A Model for Investigating Epigenetics and Eukaryotic Gene Regulation in Plants." *Biochimica et Biophysica Acta BBA—Gene Structure and Expression* 1769: 269–275.

Sung, S., and R. M. Amasino. 2004. "Vernalization in *Arabidopsis thaliana* Is Mediated by the PHD Finger Protein VIN3." *Nature* 427: 159–164.

Thomas, C. L., N. S. Graham, R. Hayden, et al. 2016. "High-Throughput Phenotyping (HTP) Identifies Seedling Root Traits Linked to Variation in Seed Yield and Nutrient Capture in Field-Grown Oilseed Rape (*Brassica napus* L.)." *Annals of Botany* 118: 655–665.

Valot, B., O. Langella, E. Nano, and M. Zivy. 2011. "MassChroQ: A Versatile Tool for Mass Spectrometry Quantification." *Proteomics* 11: 3572–3577.

Vartanian, N., P. Hervochon, L. Marcotte, and F. Larher. 1992. "Proline Accumulation During Drought Rhizogenesis in *Brassica napus var. oleifera*." *Journal of Plant Physiology* 140: 623–628.

Wood, C. C., M. Robertson, G. Tanner, W. J. Peacock, E. S. Dennis, and C. A. Helliwell. 2006. "The *Arabidopsis thaliana* Vernalization Response Requires a Polycomb-Like Protein Complex That Also Includes VERNALIZATION INSENSITIVE 3." *Proceedings of the National Academy of Sciences* 103: 14631–14636.

Xu, E., Y. Liu, D. Gu, et al. 2024. "Molecular Mechanisms of Plant Responses to Copper: From Deficiency to Excess." *International Journal of Molecular Sciences* 25: 6993.

Xu, G., X. Fan, and A. J. Miller. 2012. "Plant Nitrogen Assimilation and Use Efficiency." *Annual Review of Plant Biology* 63: 153–182.

Yokoyama, R. 2024. "Evolution of Aromatic Amino Acid Metabolism in Plants: A Key Driving Force Behind Plant Chemical Diversity in Aromatic Natural Products." *Philosophical Transactions of the Royal Society of London. Series B, Biological Sciences* 379: 20230352.

Zhu, J., K.-X. Zhang, W.-S. Wang, et al. 2015. "Low Temperature Inhibits Root Growth by Reducing Auxin Accumulation via ARR1/12." *Plant & Cell Physiology* 56: 727–736.

Supporting Information

Additional supporting information can be found online in the Supporting Information section.